

1 Yeast interaction on Chardonnay wine composition: impact of strain and inoculation time

2
3 Roullier-Gall C^{1*}, Bordet F¹, David V¹, Schmitt-Kopplin P^{2,3} and Alexandre H¹.

4
5 ¹ UMR PAM Université de Bourgogne/AgroSup Dijon, Institut Universitaire de la Vigne et du Vin, Jules
6 Guyot, Dijon, France

7 ²Comprehensive Foodomics Platform, Chair of Analytical Food Chemistry, Technische Universität München,
8 Freising, Germany

9 ³ Research Unit Analytical BioGeoChemistry, Department of Environmental Sciences, Helmholtz Zentrum
10 München, Neuherberg, Germany

11 *Corresponding author: chloe.roullier-gall@u-bourgogne.fr

12
13 Abstract

14
15 It is of great importance to understand the molecular characteristics and substantial chemical
16 transformations due to yeast-yeast interaction. Non-targeted metabolomics was used to unravel must in
17 fermentation composition, inoculated with non-*Saccharomyces (NS)* yeasts and *Saccharomyces cerevisiae*
18 (*S*) for sequential fermentation. ultrahigh-resolution mass spectrometry was able to distinguish thousands
19 of metabolites and provides deep insights into grape must composition allowing better understanding of
20 the yeast-yeast interactome. The dominance of *S*, characterized by a metabolic richness not found with *NS*,
21 is dependent on inoculation time and on the yeast species present. Co-inoculation leads to the formation
22 of new compounds, reflecting a reshuffling of yeast metabolism linked to interaction mechanisms. Among
23 the modifications observed, metabolomic unravels deep changes in nitrogen metabolism due to yeast-
24 yeast interactions and suggests that the redistribution pattern affects two different routes, the pentose
25 phosphate and the amino acid synthesis pathways.

26
27 Keys words: yeast-yeast interaction; sequential fermentation; inoculation time; metabolomics; Chardonnay
28 wine

29
30 1 Introduction

32 Grape must and wine are especially interesting models for considering interactions between
33 microorganisms as they represent a complex microbial ecosystem containing a mixture of different species
34 and strains (Barata et al., 2012). There are many different yeast species typically reported to be associated
35 with the winemaking process but many of them have been studied in the context of spoilage (Morata et
36 al., 2020; Padilla et al., 2016). However, it seems that non-*Saccharomyces* (*NS*) species can have a powerful
37 effect on aroma and flavor formation in wine (Balmaseda et al., 2021; Morata et al., 2020; Sadoudi et al.,
38 2012). The interest for *NS* species is therefore growing, especially for *Torulaspora Delbrueckii* (*D*),
39 *Starmerella Bacillaris* (*B*), and *Metschnikowia pulcherrima* (*P*) (Bordet et al., 2020; Morata et al., 2020;
40 Padilla et al., 2016). An increase in volatile esters has been reported by Renault et al. (2015), using a strain
41 of *D* to obtain more fruity wines (Renault et al., 2015). In addition to its high production of glycerol, *B* is
42 also able to produce aromatic molecules such as lactone, norisoprenoids and terpenols (Sadoudi et al.,
43 2012), as these compounds are characterized as contributing fruity and floral notes to wine. The interest
44 for *NS* yeasts in winemaking is considerable, however, compared to *S*, the number of studies remains low.
45 Most of the studies still focus on the improvement of aromas using targeted chemical analysis or sensory
46 analysis. *NS* yeasts definitely contribute to the aromatic complexity of the wine (Balmaseda et al., 2021;
47 Jolly et al., 2014; Morata et al., 2020), but the metabolite composition of wines is also of great interest as it
48 can be substantially modified depending on the presence or absence of other microbes (Liu et al., 2016;
49 Roullier-Gall et al., 2020; Sadoudi et al., 2012). Metabolomic appear as an irreplaceable tool for the
50 sensitive analysis of complex samples on a molecular level. In recent years, ultrahigh-resolution mass
51 spectrometry has prevailed as a method of choice in the compositional characterization of utmost complex
52 samples in many scientific disciplines and seems essential for understanding the changes observed linked
53 to interaction mechanisms (Bordet et al., 2020; Petitgonnet et al., 2019; Roullier-Gall et al., 2020).

54
55 Individual microorganisms are known to interact with each other, and the types of interaction encountered
56 in mixed populations of microorganisms can be positive, neutral, or even negative. Interactions are usually
57 classified as yeast-yeast cell contact, antimicrobial compounds, competition for substrates, the influence of
58 interactions in gene expression and enzymatic activities, negative-, synergistic- and additive-effect (Ciani &
59 Comitini, 2015). The most obvious example in terms of inhibitory interactions mediated by metabolites with
60 toxic effects is the production of ethanol by *S* above a concentration of 5 to 7% (Heard & Fleet, 1988). The
61 high level of alcohol produced by *S* is the main factor responsible for the dominance of *S* over other *NS*
62 yeasts (Combina et al., 2005). Other factors can lead to selective pressure, in addition to ethanol, including
63 medium-chain fatty acids, acetic acid and even oxygen availability (Fleet, 2003). Recently, antimicrobial
64 peptides corresponding to a fraction of glyceraldehyde 3-phosphate dehydrogenase enzyme have been
65 described as natural biocide secreted by one of the populations present during fermentation (Branco et al.,

2017). It has been reported that some aromatic alcohols such as tryptophol and 2-phenylethanol are used as signal molecules under certain environmental conditions (Avbelj et al., 2016).

Several studies have shown that contact between *NS* and *S* leads to the early death of the *NS* strain, which has not been observed in the context of physical separation of the two populations by different systems such as dialysis membranes (Renault et al., 2013). However, Kemsawasd et al. suggested that cell contact is combined with the secretion of antimicrobial peptides inducing the same phenomenon (Kemsawasd et al., 2015). A recent study of sequential fermentation inoculated with *T* and *S*, conducted with and without cell-cell contact between the two species, showed that cell-cell contact not only affects cell viability but also significantly affects yeast metabolism including volatile and non-volatile profiles (Petitgonnet et al., 2019).

The dynamics of the activity, growth, survival and death of microorganisms during alcoholic fermentation have been the subject of many works (Liu et al., 2017). It has been widely described that the growth kinetics of *NS* in mixed cultures are different from those in simple cultures (Bagheri et al., 2017; Petitgonnet et al., 2019; Roullier-Gall et al., 2020; Sadoudi et al., 2012; Wang et al., 2016). Two different types of yeast inoculation are generally considered in mixed fermentation: co-inoculations and sequential inoculations (Beckner Whitener et al., 2016). Co-inoculation is the simplest way of proceeding in winemaking since all yeasts are added to the must at the same time. In contrast, sequential inoculation requires two distinct steps. *NS* yeasts are added to the must and begin fermentation alone. After a defined period, the *S* yeasts are then added to complete the fermentation. Several authors agree that sequential culture or mixed culture impacts the sensory characteristics of wine (Curiel et al., 2017). According to Wang et al., mixed culture could result in the reduction or disappearance and loss of viability of *NS* yeasts (Wang et al., 2016). The variance between wine from sequential and mixed cultures reflects differences at the yeast metabolic level which have been rarely studied. The whole point of metabolomics is the possibility to study the differences induced by yeast interaction, which in addition can provide information on the nature of the interactions (Roullier-Gall et al., 2020). Although their implementation is more complex, sequential inoculations are particularly interesting because they provide good control over the evolution of fermentation. In this study, the sequential inoculation approach was selected to test the impact of the time of adding *S* on the wine metabolome fermented by three different *NS* yeasts.

2 Material and Methods

2.1 Yeast strains

Three *NS* yeast strains were obtained from the collection of the Burgundy University Vine and Wine Institute. The strains selected for this study were *Starmerella Bacillaris* (*B*), *Torulaspota delbrueckii* (*D*), *Metschnikowia*

99 *pulcherrima* (P) and a commercial strain of *Saccharomyces cerevisiae* (S) used as a reference for sequential
100 inoculation (Supplemental Figure 1). All the yeast strains were grown at 28°C in modified YPD medium (20
101 g.L⁻¹ glucose, 10 g.L⁻¹ peptone and 5 g.L⁻¹ yeast extract with 20 g.L⁻¹ of agar for Petri dish cultivation),
102 supplemented with 0.2 g.L⁻¹ of chloramphenicol. The yeasts were pre-cultured in 250 mL sterile Erlenmeyer
103 flasks, closed with dense cotton plugs, containing 150 mL of modified YPD medium under agitation (100 rpm)
104 at 28°C for 24h.

105 106 2.2 Enumeration of Microorganisms

107 After yeast growth in YPD medium, 2 microtubes containing one milliliter of yeast culture with 10⁶ cells
108 were centrifuged (9000g for 5min). The pellet was suspended in 1mL of in MacIlvaine's buffer (0.1 M citric
109 acid, 0.2 M disodium hydrogen phosphate; pH 4). The first tube was used as control. The second tube was
110 complemented with 2 µL of the viability probe 5-CFDA, AM (5-carboxyfluorescein diacetate, acetoxymethyl
111 ester; Thermo Fisher Scientific) to achieve a final concentration of 1.5 mM incubated for 25 min in
112 darkness at room temperature before flow cytometry (FCM) analysis. The FCM analysis was performed
113 with a BD Accuri C6 flow cytometer. The 5-CFDA (second tube) was excited by the flow cytometer laser at
114 488 nm and emitted green fluorescence collected by the filter: 530 nm +/- 15nm (FL1 channel). The results
115 were compared to the control tube to eliminate cellular autofluorescence. The data were analyzed using
116 statistical tables that indicate the number and percentage of viable cells as well as fluorescence intensity.

117 118 2.3 Fermentations

119 Fermentations were carried out in duplicate in white must (Chardonnay from Marsannay in France)
120 containing 212 g.L⁻¹ of glucose/fructose, a pH of 3.24 and 291 mg.L⁻¹ of assimilable nitrogen. The must was
121 centrifuged at 7,000 g for 7 min at 4°C. Sugar concentration and ethanol production were monitored by
122 Fourier transform infrared spectroscopy (FTIR, OenoFOSS™, FOSS, Hilleroed, Denmark). Pure and
123 sequential fermentations were carried out in 250 mL Erlenmeyer flasks, closed with sterile cotton wool,
124 and containing 100 mL of white must. Pure fermentations were inoculated with pre-cultured yeast cells 10⁶
125 cells.mL⁻¹ and incubated at 20°C without agitation (B, D, P and S). Sequential fermentations were
126 inoculated with 10⁶ cells.L⁻¹ NS yeast (B, D or P). A second inoculation with 10⁶ cells.mL⁻¹ S was performed
127 24 h (BS24h, DS24h and PS24h), 48h (BS48h, DS48h and PS48h) and 72h (BS72h, DS72h and PS72h) after
128 the NS yeast inoculation.

129 130 2.4 Direct infusion FT-ICR-MS

131 Ultrahigh-resolution FT-ICR-MS was performed with a 12 T Bruker Solarix mass spectrometer (Bruker
132 Daltonics, Bremen, Germany) equipped with an APOLLO II electrospray source in negative ionization mode.

133 For the MS analysis, the samples were diluted at 1:100 (v/v) in methanol (LC-MS grade, Fluka, Germany).
134 The diluted samples were infused into the electrospray ion source at a flow rate of 120 $\mu\text{L}\cdot\text{h}^{-1}$. The settings
135 for the ion source were: drying gas temperature 180 °C, drying gas flow 4.0 $\text{L}\cdot\text{min}^{-1}$, capillary voltage 3,600
136 V. The spectra were first calibrated externally by ion clusters of arginine (10 ppm in methanol). The internal
137 calibration of each spectrum was conducted with a reference list including selected wine makers and
138 ubiquitous fatty acids (Roullier-Gall et al., 2014). The spectra were acquired with a time-domain of 4
139 megawords and 400 scans were accumulated within a mass range of m/z 92 to 1000. A resolving power of
140 400,000 at m/z 300 was achieved. Raw spectra were post-processed by Compass DataAnalysis 4.2 (Bruker
141 Daltonics, Bremen, Germany) and peaks with a signal-to-noise ratio (S/N) of at least 6 were exported to
142 mass lists. All exported m/z features were aligned into a matrix containing averaged m/z values (peak
143 alignment window width: ± 1 ppm) and the corresponding peak intensities of all the samples analyzed.
144 Molecular formulas were assigned to the exact m/z values by mass difference network analysis using a
145 software tool developed in-house. In total, 3920 detected features could be assigned to distinct and
146 unique molecular formulae. More than 95% of all assignments were found within an error range lower
147 than 0.2 ppm. All further calculations and filtering were performed with Perseus 1.5.1.6 (Max Planck
148 Institute of Biochemistry, Germany) and R Statistical Language (version 3.1.1).

150 **3 Results and discussion**

151
152 Chardonnay must was divided into 26 aliquots, two were inoculated with pure culture of *S*, eight with *B*,
153 eight with *D* and eight with *P* (supplemental Figure 1). Every 24 hours, *S* was added to two aliquots of each
154 *NS* pure culture (*B*, *D* and *P*) to promote the impact of addition time on sequential fermentation. Different
155 sequential times (24, 48 and 72 hours) were chosen to avoid the rapid dominance of *S*. Samples were
156 collected and analyzed 24, 48, 72 and 96 hours after the beginning of fermentation and at the end of the
157 alcoholic fermentation (corresponding to glucose/fructose concentration lower than $2\text{g}\cdot\text{l}^{-1}$).

159 **3.1 Impact of type of yeast and sequential fermentation on classical oenological parameters**

160
161 At the end of alcoholic fermentation, all the sequential *S* had an ethanol concentration between 9.0 and
162 11.5% (v/v) and a sugar concentration lower than $2.0\text{g}\cdot\text{l}^{-1}$. The samples inoculated with *P* took the longest
163 to finish fermentation with at least 12 days in contrast with the pure culture for incomplete alcoholic
164 fermentation. For other *NS* yeasts seven days were enough to complete alcoholic fermentation while it
165 took five days in the case of *S* pure culture (Supplemental Figure 2). Sequential fermentation helps to
166 increase the ethanol concentration but also to reduce the fermentation time compared to *NS* pure culture

167 fermentation. This is especially obvious when *S* is added early in the fermentation process (supplemental
168 Figure 2 and supplemental Table 1). The decrease in the wine alcohol content from sequential
169 fermentation when compared with *S* pure culture confirmed the utility of *NS* yeast for reducing the
170 ethanol content. For example, *P* pure culture did not exceed an ethanol concentration of 7.8% (v/v) at the
171 end of fermentation (while *S* pure culture reached 11.5%), but reached 9.6%, 10.2% and 10.6% when *S* was
172 added after 72h, 48h and 24h fermentation, respectively (Supplemental Figure 2 and supplemental Table
173 1). Thus, the earlier *S* is added in the process, the faster the alcoholic fermentation and the higher the
174 ethanol concentration reached. Other classical oenological parameters such as malic acid, volatile acidity
175 and total acidity were also impacted by yeast type and sequential fermentation (supplemental Table 1). As
176 the must and the fermentation conditions were the same for all modalities, differences detected in the
177 final wines compositions and highlight using metabolomics were induced by the type of yeast, the
178 interaction between yeast and the time of *S* addition.

180 3.2 Single yeast fermentation markers

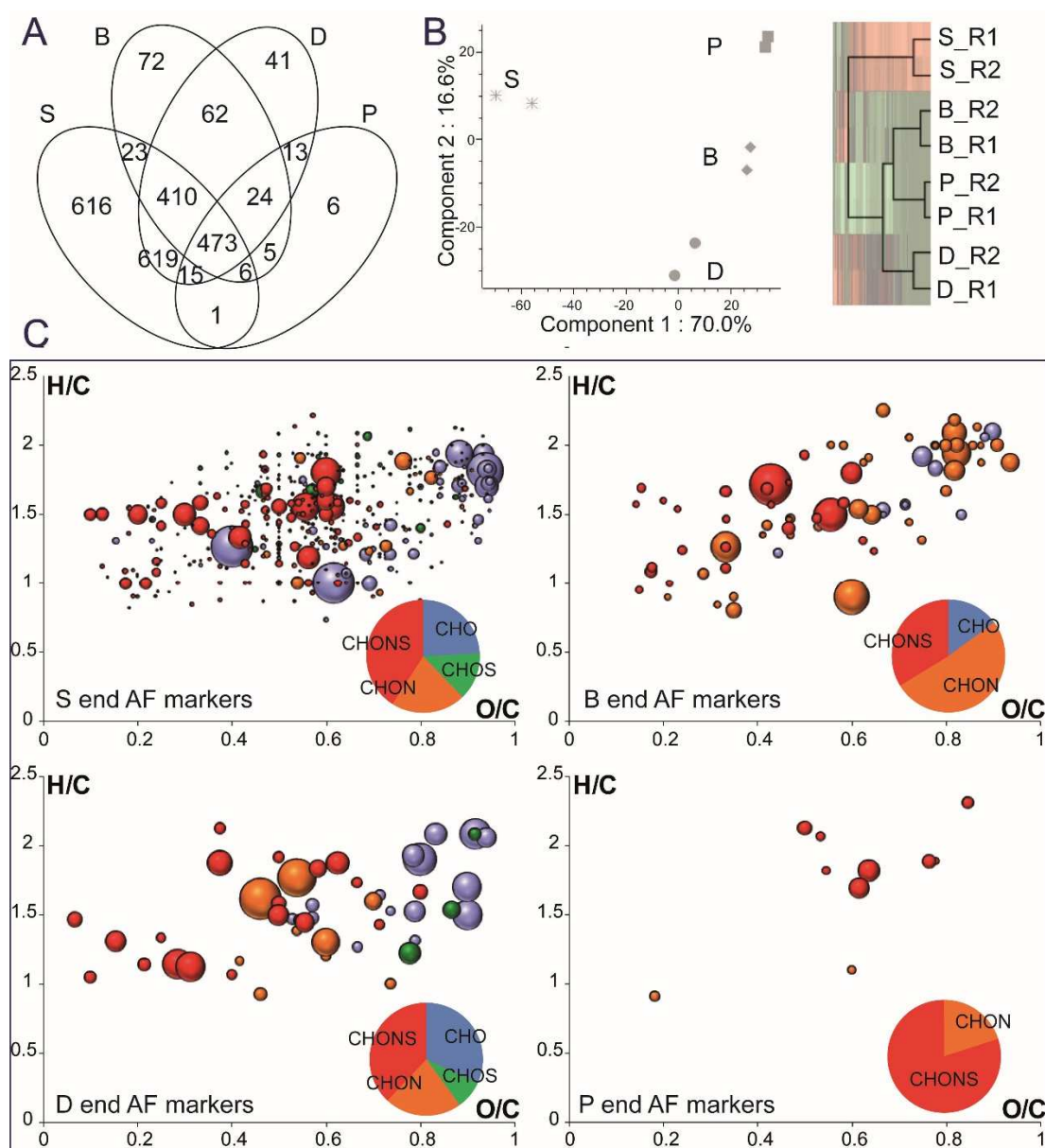
181
182 Non-targeted direct infusion ultrahigh-resolution mass spectrometry analyses of wines from *S* and each *NS*
183 yeast fermentation were performed at the end of alcoholic fermentation. While the wide range of chemical
184 properties often complicates simultaneous and comprehensive analysis of wine and must, FT-ICR-MS was
185 able to distinguish more than 2000 compounds produced during fermentation. The spectra acquired allowed
186 annotating 2163, 1107 1657 and 759 molecular formulas composed of carbon, hydrogen, oxygen, sulfur, and
187 nitrogen in *S*-, *B*-, *D*- and *P*- wines, respectively (Supplemental figure 3). Differences in composition between
188 wines from *S*, *B*, *D* and *P* could be visualized by comparing raw spectra and are highlighted in the Venn
189 diagram (Figure 1 and supplemental Figure 3). The Venn diagram allows the extraction of 616, 72, 41 and 6
190 compounds which could be detected exclusively in *S*-, *B*-, *D*- and *P*- wines, respectively (Figure 1). Around
191 31% of the total composition was unique to one of the wine groups and *S* wines presented the highest
192 number of unique compounds, amounting to 26% of the total composition as unique. These results are
193 rather original, as volatile compounds are usually analysed for yeast strain distinction and, as far as we know,
194 there is no specific aromatic compound linked to one yeast species. Indeed, the differences due to yeast in
195 previous studies were only quantitative (Bordet et al., 2020; Del Fresno et al., 2017). Whereas, wines
196 fermented by *NS* yeasts have mainly been characterized up to now by their volatile profiles, here we confirm
197 the power of the metabolomic approach for in-depth differentiation between species, as demonstrated in
198 our previous results (Roullier-Gall et al., 2020).

199 Metabolomics is a powerful tool capable of highlighting interspecies differentiation and it also gives details
200 regarding the nature of the differences. Indeed, *NS* species lead to different wine compositions including

201 unique metabolites (Supplemental Figure 3). Despite these differences in composition, a large part of wine
202 chemical composition is common to at least two wine groups at the end of alcohol fermentation (1651
203 metabolites representing 69% of the total composition) and 473 metabolites are present in all four groups
204 of wine (20% of the total composition) (Figure 1 and supplemental Figure 3). The annotation of these
205 metabolites covered all the main classes of primary and secondary metabolites including for example
206 carbohydrate, amino acids, organic and fatty acids, nucleotides, vitamins, organosulfur and flavonoid.
207 However, a large proportion of these common compounds are present at different intensities which means
208 at different concentrations. Putative annotated glutaryl-glycine (level 3), was detected in *S*, *B* and *D* wines at
209 similar intensity whereas malic acid (level 1) was detected in all four groups of wines but present differences
210 in term of concentration (5.2 g/L for *S*, 4.9 for *B*, 6.4 for *D* and 6.3 for *P* - Supplementary table 1). Finally, only
211 a small part of the composition of the wine samples is present at exactly the same concentration in all the
212 wines (Supplemental Figure 3).

213
214 The principal component analysis (PCA) of pure culture wines at the end of alcoholic fermentation
215 confirmed the huge difference in terms of non-volatile composition between *S* wines and *NS* wines (Figure
216 1). The first component of the PCA explained 70% of the variability between the samples and opposed *S*
217 and *NS* wines. The second component of the PCA explained 16.6% of the variability and highlighted
218 differences between chemical compositions *P*, *B* and *D*. Hierarchical cluster analysis (HCA) confirmed
219 previous results and highlighted the greater proximity between the compositions of *B* and *P* wines. These
220 results reflect considerable differences in yeast metabolism between species, thereby supporting previous
221 analyses (Balmaseda et al., 2021; Rollero et al., 2021). To characterize the impact of yeasts on final wine
222 composition, we computed ANOVA statistics and retrieved a subset of features that showed significant
223 differences in their mean peak intensities (p -value < 0.05) between *S*, *B*, *D* and *P* wines. These extracted
224 features can be used as markers to distinguish and characterize wines depending on the yeast used for the
225 fermentation. 449, 146, 163 and 13 markers were statistically extracted for *S*, *B*, *D* and *P* wines respectively
226 and represented in van Krevelen diagrams (Molecular formulas composed by elements C, H, O, N and S,-
227 Figure 1). The highest number of markers was found for *S* wines (449 markers), confirming the massive
228 impact of *S*, which agrees with previous PCA and HCA. *S* markers are composed of 24% CHO, 14% CHOS,
229 21% CHON and 41% CHONS compounds located in the van Krevelen diagram, where carbohydrate-,
230 polyphenol- and amino acid-derivatives are expected. For example, out of the 449 markers from *S* wines,
231 only 32 were putatively annotated (level 3) in known databases. On the 32 annotated compounds, 20 were
232 identify as peptides, one as sulfur containing compounds (vanillic acid sulfate – annotation level 3) and 11
233 CHO containing compounds. By comparison, *B* markers do not contain any CHOS compounds but are
234 mainly composed of CHON compounds (53%) in the area where amino acid and peptide-like compounds

235 are expected, while *P* markers contain only nitrogen containing compounds (CHON in orange and CHONS in
 236 red) (Figure 1). The differences in terms of composition, especially regarding nitrogen compounds (amino
 237 acids and peptides), reflect different species dependent yeast metabolisms. For example it has been
 238 reported that the low consumption of amino acids by *B* seems to be a specific feature of this species
 239 (Englezos et al., 2018; Gobert et al., 2017). Furthermore, it has been shown that *B* can excrete amino acids
 240 during fermentation, including branched amino acids. The fact that *P* markers mainly contain nitrogen
 241 containing markers reflects either a low nitrogen uptake by this species (Roca-Mesa et al., 2020) or/and its
 242 known protease activity (C. Snyman et al., 2019). The fact that no CHOS markers were found in *B* might
 243 reflect differences in sulfur compound metabolism and point to new studies.



244
 245 **Figure 1:** A: Venn diagrams, B: principal component analysis and hierarchical cluster of wines from single
 246 yeast fermentations (*S*, *B*, *D* and *P*) at the end of alcoholic fermentation. The first two components
 247 represent 86.6% of the variability. The cluster analysis followed by an ANOVA with t-test (p-value 0.05)
 248 allows the extraction of specific masses for each single fermentation highlighted in C: the van Krevelen

249 diagrams. Bubble sizes in the van Krevelen diagrams indicate relative intensities of corresponding peaks in
250 the spectra and bubble colors represent chemical composition with CHO containing compounds
251 represented in blue; CHOS in green; CHON in red and CHONS in orange.

252

253 3.3 Metabolic changes during the early stage of alcoholic fermentation

254

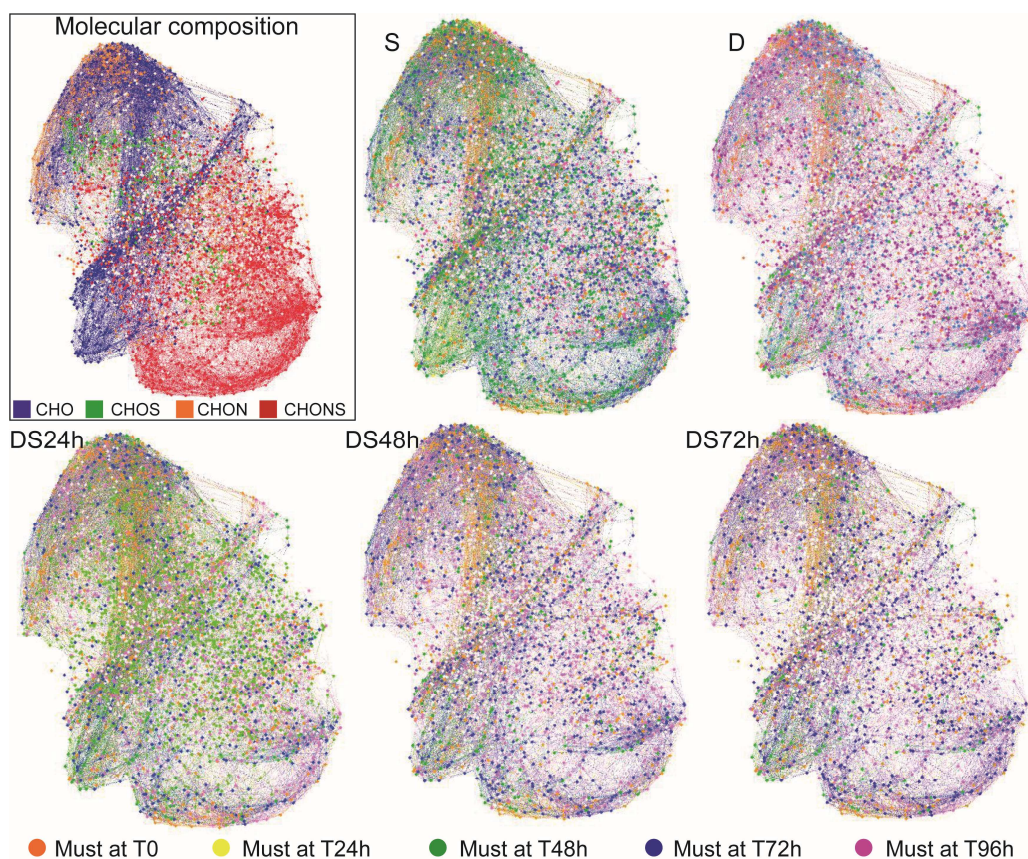
255 A mass difference network was constructed, based on composition evolution during fermentation (Figure 2
256 and supplemental Figure 4). *D* sequential fermentations (DS) are represented as examples for visualizing
257 changes in must during the early stages of alcoholic fermentation and compositional modulation due to
258 the time of *S* addition. The nodes represent all the assigned molecular formulas connected to each other
259 by possible chemical transformations during alcoholic fermentation. Using networks, it is possible to make
260 links between the compounds detected (Supplemental Figure 4). It was possible to connect 75% of the
261 annotated compounds using 172 biochemical transformations. For example, hydroxylation (or de-
262 hydroxylation) characterized by a difference between two compounds by an oxygen (+/- O) allows
263 connecting 793 couples of compounds. Hydrolysis or condensation (+/- H₂O) allows connecting 423 couples
264 of compounds, glycine condensation (+/- C₂H₃ON) connected 139 couples of compounds and pyruvic acid
265 decarboxylative addition (+/- C₂H₄O) connected 57 couples of compounds. Networks are colored according
266 to the detection time (24h, 48h, 72h and 92h) of compounds during must fermentation for each pure (*S*
267 and *D*) and sequential fermentation (DS24h, DS48h and DS72h). Networks highlight a clear difference in
268 day-to-day composition between yeast strains (Figure 2). The number of metabolites detected drastically
269 increases with fermentation time. Indeed, the number of compounds started with 388 in must before
270 yeast addition and increased to 1351 compounds for *S* must and 566 for *D* must in pure culture after 48h
271 fermentation and 2705 for *S* must and 1930 for *D* must after 96h fermentation (Table 1). A large number of
272 compounds appeared during the first two days of *S* fermentation, with 936 new compounds detected after
273 48h fermentation (in green) and another 1003 compounds after 72h (in blue), as detailed in Table 1. In
274 contrast, *D* fermentations presented a slower evolution with 546 new compounds detected after 72h
275 fermentation (in blue) and 818 new compounds formed after 96h (in pink). To complete the analysis and
276 statistically quantify the differences in metabolite composition in the fermenting musts, principal
277 component analysis was used. PCA score plots show clear differences in fermentation dynamics between
278 yeast type (*S* versus *NS*), type of fermentation (pure culture vs sequential fermentation) and time of *S*
279 addition in the case of sequential fermentation (24h vs 48h vs 72h) (Supplemental Figure 5, 6 and 7). Based
280 on PCA including all the samples from pure culture (*S*, *D*, *B* and *P*), fermenting musts were rapidly

281 segregated. For example, after 48 hours fermentation, it was already possible to distinguish the *S* and *D*
282 yeasts based on their metabolic profile (C1 explained 58.2% of the variability –Supplemental Figure 5).

283
284 In sequential fermentation the influence of *S* on chemical composition was already visible 48h after its
285 addition (separation from pure culture in PCA). The distinction between pure culture and sequentially
286 fermented must was even more noticeable after 96 hours fermentation, regardless of the *NS* yeast species
287 (Supplemental Figures 5, 6 and 7). The dominance of *S* is extremely rapid and confirmed the excellent
288 adaptation of *S* along the fermentation process. To illustrate this, the PCA showed that the sequential
289 culture of *P* (PS24h) was separated from the pure cultures of *P* by the first component (C1) which
290 represented 91.0% of variability 96h after the beginning of fermentation (Supplemental Figure 6). The
291 same observation was true for the other sequential cultures like BS24h (C1: 77.9% - supplemental Figure
292 7). Furthermore, when *S* was added 24 hours after the start of *D* fermentation, *S* completely dominated
293 the medium 48 hours after its addition, making it possible to distinguish the sequential culture of *D* alone.
294 The impact of *S* was stronger with early *S* addition. The addition of *S* after 72h fermentation, at DS72h for
295 example, did not impact the composition dynamics as much as for DS24h. Indeed, adding *S* after 24h and
296 48h fermentation increased the number of new compounds formed (+201 at 48h; +820 at 72h for DS24
297 and +705 at 72h for DS48) while the addition of *S* after 72h fermentation contributed fewer newly formed
298 metabolites (Table 1). The metabolic richness of *S* was much higher than that of *D* which itself was higher
299 than that of *B* which was richer than *P*. The composition of the must evolved rapidly in the presence of *S*,
300 while the presence of *P* had a lower impact over fermentation time, which reflected a lower metabolic
301 activity specific to *P*.

302
303 The number and the type of compounds detected after 96h fermentation showed that a must fermented
304 by a single yeast (*NS* or *S*) has a final composition distinct from the same must fermented by a combination
305 of yeasts (BS, DS and PS). Indeed, the inoculation of *S* for sequential fermentation after 24h fermentation
306 drastically changed the fermentation dynamics and increased the number of newly formed compounds.
307 Thus, sequential DS24h fermentations were closer to the composition dynamics of *S* than to *D* in pure
308 culture, confirming the rapid dominance of *S* over *D*. From the metabolomic viewpoint, these results
309 confirm the ability of *S* to outcompete other microbial species during alcoholic fermentation processes
310 (Albergaria & Arneborg, 2016). The metabolite composition of DS24 was close to that of pure *S*,
311 demonstrating that despite the development of *D* 24h before the addition of *S*, once inoculated, *S* could
312 displace *D*. This ability is linked to its higher fermentation fitness compared to other species (Williams et
313 al., 2015) and to interactions between these microorganisms (Bordet et al., 2020). Our results demonstrate
314 that *S* took over from *D* due to its competitive capacity and physiological fitness. They also clearly show the

315 existence of negative interactions between these species, confirming previous results (Albergaria &
 316 Arneborg, 2016). This highlights that metabolomics is an interesting tool for unraveling yeast interaction
 317 and studying yeast dominance.



318
 319 **Figure 2:** Mass difference network based on the evolution of composition during fermentation in samples
 320 *D*, *S* and *DS*. 75.0% of assigned molecular formulas could be connected in the network by allowing a set of
 321 172 biological transformations. The transformations are non-directed and correspond to edges in the
 322 graph. The compounds correspond to nodes in the graph. In the first networks, nodes are colored
 323 according to their chemical composition: CHO in blue, CHOS in green, CHON in orange and CHONS in red.
 324 In the other five networks, nodes are colored according to their detection time during fermentation.
 325 Compounds already present in must are represented in orange, then compounds detected after 24h
 326 fermentation are represented in yellow, after 48h in green, after 72h in blue and after 96h in purple.

327
 328 **Table 1:** Compounds detected in the initial must and new compounds detected at 24h, 48h, 72h and 96h
 329 after the beginning of alcoholic fermentation in samples from fermentations *D*, *S* and *DS*.

	S	DS24h	DS48h	DS72h	D
0h	388	388	388	388	388
24h	27	6	6	6	6
48h	936	201	172	172	172

72h	1003	820	705	546	546
96h	351	611	443	563	818
Total	2705	2026	1834	1675	1930

330

331

332 3.4 Impact of *S* addition time on the final wine

333

334 Depending on the yeast and fermentation type (sequential or pure culture fermentation), the evolution of
335 composition during alcoholic fermentation did not lead to the same final wine composition. Hierarchical
336 cluster analyses (HCA) that included all fermentation conditions for each *NS* yeast at the end of the
337 alcoholic fermentation were performed (Figure 3). HCA confirmed that *NS* wines in single or sequential
338 fermentation and *S* wines presented a different composition at the end of fermentation with excellent
339 separation. Sequential fermentation with the addition of *S* at 24h appeared to have the exo-metabolome
340 closest to *S* regardless of the *NS* yeast used for fermentation (*D*, *B* or *P*). These results highlight that the
341 addition time of *S* (24h vs 48h vs 72h) significantly impacts the wine exo-metabolome. The greater
342 proximity between wine from *S* fermentation and sequential fermentation at 24h compared to *NS* single
343 fermentation indicated the rapid dominance of *S* over *NS*, resulting in a high number of unique metabolites
344 and higher intensities of compounds when *S* is added shortly after the beginning of fermentation
345 (Supplemental Figures 8, 9 and 10). Conversely, sequential fermentation when *S* is added at 48h and 72h
346 showed a better balanced impact between *S* and *NS* on the final composition, with a new profile including
347 compounds from *S* and *NS* with compounds unique to sequential fermentation (Supplemental Figures 8, 9
348 and 10). Compounds whose intensity varied significantly (ANOVA with p value 0.05) according to the *S*
349 addition time were then extracted and represented in Van Krevelen diagrams together with a pie chart
350 indicating the composition of the molecular formulas (Supplemental Figures 8, 9 and 10). Each metabolite
351 was classified depending on the composition of their formula into one of the principal chemical families
352 including amino acid and peptides, amino sugars, carbohydrate, lipids, nucleotides, polyphenolic
353 compounds and derivatives and unknown compounds. The highest intensity *S* metabolites with an
354 intensity decreasing from *S* to DS72, DS48, DS24h and *D* were composed of a relative equivalent number of
355 CHO (blue) and CHONS (red) compounds in the mass range of 350-550 Da and mostly annotated as
356 peptides (22.9%), carbohydrate (21.8%), lipids (11.45%) and polyphenolic compounds (9.9%) using
357 metabolomic pathways (Supplemental Figure 8). Conversely, compounds higher in intensity in *D* wines,
358 with an intensity decreasing from *D* to DS24, DS48, DS72h and *S*, were composed of a large proportion of
359 CHONS (red) compounds in the mass range of 250-400 and 450-550 Da and mostly identified as amino
360 sugars (26.2%), peptides (24.8%) and carbohydrate (24.3%).

361

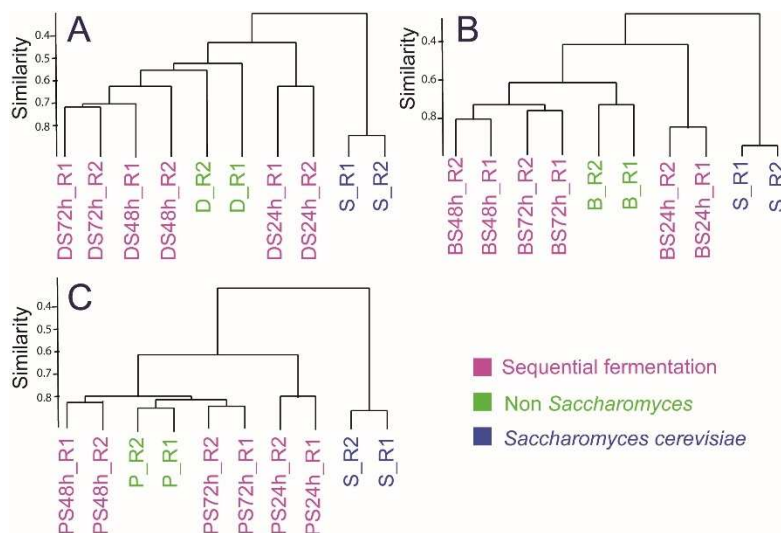
362 To go further, all the sequential fermentations were compared to corresponding *S* and *NS* pure culture
363 wine (*NS/NS24h/S*, *NS/NS48h/S* and *NS/NS72h/S*) to focus on the impact of time of *S* inoculation on the
364 final wine composition (Figure 4). First, hierarchical cluster analyses were performed and highlighted
365 compositional differences. As in figure 3, whatever the couple of wines considered, higher profile similarity
366 was always found between the *NS* and sequential fermentation (Supplemental Figure 12). Secondly, Venn
367 diagrams were used to extract compounds at each fermentation and the common metabolites, which were
368 further represented in plots representing the distribution of chemical families (CHO, CHOS, CHON and
369 CHONS) and potential molecular families (Figure 4). The association of both yeast species shows the
370 modification of the exo-metabolome which clearly differs from that of *NS* and *S*, and even differs from the
371 addition of the *NS* and *S* metabolomes. Indeed, part of the composition of *NS* and *S* was not found in wines
372 obtained from sequential fermentation and part of the composition of wine obtained from sequential
373 fermentation was unique, confirming interaction between yeasts in sequential fermentation. Such
374 observations have been reported for volatile compounds. Previous studies reported that mixed
375 fermentation resulted in unique volatile profiles that differed from single strain fermentations (Morgan et
376 al., 2020). However, the specific exo metabolomic pattern reported here confirmed what has been found
377 for volatile profiles and supports the view that in mixed fermentation, the metabolic fingerprint is linked to
378 yeast-yeast interaction and not solely to the addition of the exo metabolome of each single strain.

379

380 Focusing on the number of unique compounds found in sequential fermentation, 10 to 20 unique
381 metabolites were highlighted for *DS* wines depending on the time of *S* addition, 91 to 30 for *BS* wines and
382 105 to 24 for *PS* wines. Surprisingly, the number of unique compounds varied differently depending on the
383 couple of yeasts. Thus, higher numbers of unique compounds were found in *B* and *P* sequential
384 fermentation wines compared to *D*. Moreover, the number of unique compounds decreased with the time
385 of *S* addition in *B* and *P* but increased in *D*. These results confirm that each yeast species has a different
386 metabolism and that it is modulated based on yeast interaction during sequential fermentation.
387 Interestingly, the number of common compounds between *NS* and sequential fermentation increased with
388 the time of *S* addition from 108, 129 to 137 for *D/DS24h*, *D/DS48h* and *D/DS72h*, respectively. On the
389 contrary, the number of common compounds between *S* and sequential fermentation decreased
390 drastically with the time of *S* addition from 169, 50 to 35 for *S/DS24h*, *S/DS48h* and *S/DS72h*, respectively,
391 indicating a lower impact of *S* on the *DS* composition for the inoculation time of 72h. The same was true
392 for *B* and *BS* fermentation whereas the number of common compounds between *P* and *PS* was stable for
393 all the *S* inoculation times (24h, 48h and 72h). When *S* was added early in fermentation, its impact was
394 strong and dominant compared to that of *NS*, whereas the later *S* was inoculated, the weaker its impact on

395 the final wine composition. Annotated compounds in the biosynthesis of amino acid pathways are
 396 represented to illustrate the evolution of composition (Supplementary figure 10). Of the compounds that
 397 composed the amino acid pathways, 41 were detected in wines (in black) including five compounds
 398 detected with increasing intensity from S to D (in red). These compounds are involved in the pentose
 399 phosphate pathway, providing precursors for amino acid synthesis and for the production of polyols, which
 400 is a specific trait of D. Seven compounds were detected with increasing intensity from D to S (in blue), and
 401 all are involved in amino acid biosynthesis pathways (Supplementary figure 11). These changes reflect
 402 competition for nitrogen compounds, leading to a considerable redistribution of fluxes through the central
 403 amino metabolic network. Indeed, competition for nitrogen compounds in mixed fermentation has been
 404 reported (Rollero et al., 2021). As reported previously (Seguinot et al., 2019), competition for amino acids
 405 can lead to the depletion of certain amino acids and consequently to extensive changes in the amino
 406 metabolism network to use available nitrogen sources. This redistribution pattern might also reflect
 407 specific D nitrogen metabolism. Su et al., reported that *D* consumed nitrogen sources are mainly directed
 408 towards the de novo synthesis of proteinogenic amino acids (Su et al., 2020). Thus, our results unravel
 409 deep changes in nitrogen metabolism due to yeast-yeast interactions and suggest that the redistribution
 410 pattern affects two different routes, the pentose phosphate pathway and the amino acid synthesis
 411 pathways.

412



413

414 **Figure 3:** Hierarchical cluster of wine from single yeast fermentations (*NS* in green and *S* in blue) and
 415 sequential fermentation (in pink) with *S* added at 24h, 48h and 72h at the end of alcoholic fermentation for
 416 *T. delbrueckii* (A), *S. bacillaris* (B) and *M. pulcherrima* (C).

417

418

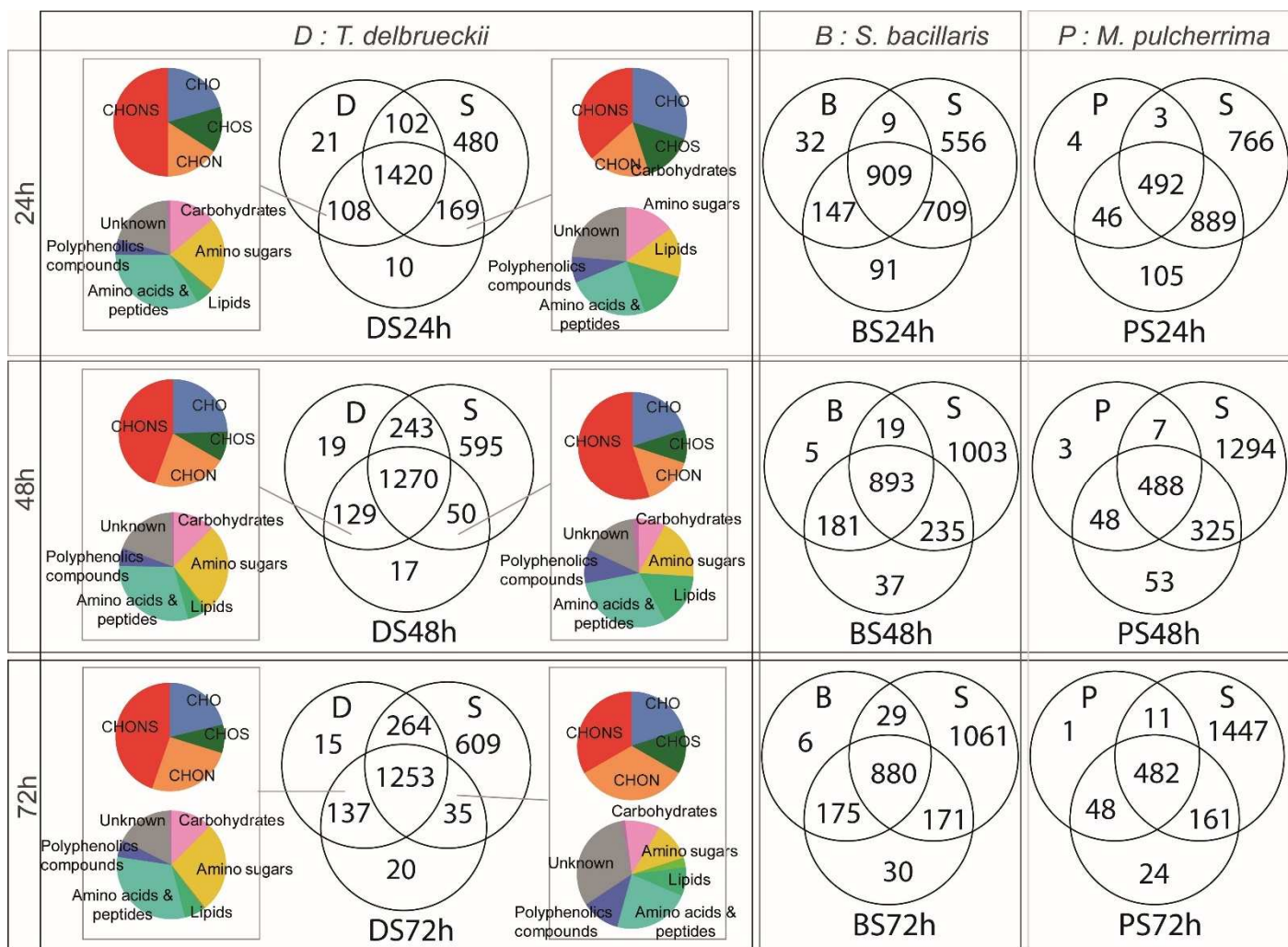


Figure 4: Venn diagrams of wine at the end of fermentation from single yeast fermentations (NS and S) and sequential fermentation with S added at 24h (NS24h), 48h (NS48h) and 72h (NS72h) with pie charts displaying the compounds common to NS and S in single and sequential fermentations based on chemical composition (CHO in blue, CHOS in green, CHON in orange and CHONS in red) and metabolic pathway (Carbohydrates in pink, amino sugars in yellow, lipids in green, amino acids and peptides in turquoise, polyphenol compounds in dark blue and unknown in grey). Compounds classified as unknown refer to compounds not annotated in metabolic pathways.

4 Conclusion

Most interaction studies, so far, focused on targeted volatile compounds analysis. However the volatile composition represents only a small part of the modification induced by fermentation. Here we focus on non-targeted ultrahigh resolution mass spectrometry, used to monitor the non-volatile compositional changes, due to yeast interactions and sequential fermentation. Thousands of compounds have been recorded simultaneously and linked to the specific presence of yeast and to their interactions. Based on the exo metabolome, wines from the 4 species could be easily distinguished, reflecting different yeast

436 metabolisms. Huge metabolic differences have been observed on a larger number than what could ever
437 recorded for volatile compounds. Each yeast led to a different wine non-volatile profile and could be
438 described by a unique pattern of metabolites. From the start of fermentation *S* was characterized by many
439 unique markers, a sign of metabolic richness not found with the other yeast strains (*B*, *D* and *P*). Some
440 strains were characterized by the absence of specific sulfur markers (CHOS) such as *B* and *P*; *P* was
441 characterized by many nitrogen and sulfur containing compounds (CHONS), signs of a specific metabolism.
442 The evolution of the must profile in sequential culture was monitored during alcoholic fermentation,
443 making it possible to demonstrate that the interactions between *S* and *NS* occurred very early, noticeable
444 24 hours after the addition of *S* in the medium. Once *S* was added in the must, the evolution kinetics of the
445 composition confirmed the metabolic richness of *S* compared to other species with an increasing number
446 of metabolites detected. The ability of *S* to dominate other species is exceptional since it marked the
447 metabolic imprint very quickly as soon as it was present in the medium. Sequential fermentations are very
448 effective in modifying the composition and the final wines are different in terms of the metabolite than the
449 simple addition of pure cultures. Indeed, markers have been highlight as unique to mixed cultures which is
450 the reflection of interactions between yeasts.

451 Nitrogen metabolism seemed to be the metabolic pathway most altered by sequential cultures, which
452 reflects yeast-yeast interactions. The redistribution pattern particularly affects two different routes, the
453 pentose phosphate pathway and the amino acid synthesis pathways. Indeed, competition for nitrogenous
454 compounds resulted in *D* by a rearrangement of nitrogen metabolism observable through the evolution of
455 must composition during sequential fermentation. To conclude, this study provides new insights on yeast-
456 yeast interactions during the alcoholic fermentation of Chardonnay must.

457 458 Funding

459 This research was funded by the Regional Council of Bourgogne- Franche-Comté, the “Fonds Européen de
460 Développement Régional (FEDER) Metabolom : BG0022832

461 462 References

- 463
464 Albergaria, H., & Arneborg, N. (2016). Dominance of *Saccharomyces cerevisiae* in alcoholic fermentation processes:
465 Role of physiological fitness and microbial interactions. *Applied Microbiology and Biotechnology*, *100*(5),
466 2035–2046. <https://doi.org/10.1007/s00253-015-7255-0>
- 467 Avbelj, M., Zupan, J., & Raspor, P. (2016). Quorum-sensing in yeast and its potential in wine making. *Applied*
468 *Microbiology and Biotechnology*, *100*(18), 7841–7852. <https://doi.org/10.1007/s00253-016-7758-3>

- 469 Bagheri, B., Bauer, F. F., & Setati, M. E. (2017). The Impact of *Saccharomyces cerevisiae* on a Wine Yeast Consortium
470 in Natural and Inoculated Fermentations. *Frontiers in Microbiology*, *8*.
471 <https://doi.org/10.3389/fmicb.2017.01988>
- 472 Balmaseda, A., Rozès, N., Leal, M. Á., Bordons, A., & Reguant, C. (2021). Impact of changes in wine composition
473 produced by non-*Saccharomyces* on malolactic fermentation. *International Journal of Food Microbiology*,
474 *337*, 108954.
- 475 Barata, A., Malfeito-Ferreira, M., & Loureiro, V. (2012). The microbial ecology of wine grape berries. *International*
476 *Journal of Food Microbiology*, *153*(3), 243–259. <https://doi.org/10.1016/j.ijfoodmicro.2011.11.025>
- 477 Beckner Whitener, M. E., Stanstrup, J., Panzeri, V., Carlin, S., Divol, B., Du Toit, M., & Vrhovsek, U. (2016). Untangling
478 the wine metabolome by combining untargeted SPME–GCxGC–TOF–MS and sensory analysis to profile
479 Sauvignon blanc co-fermented with seven different yeasts. *Metabolomics*, *12*(3), 53.
480 <https://doi.org/10.1007/s11306-016-0962-4>
- 481 Bordet, F., Joran, A., Klein, G., Roullier-Gall, C., & Alexandre, H. (2020). Yeast–Yeast Interactions: Mechanisms,
482 Methodologies and Impact on Composition. *Microorganisms*, *8*(4), 600.
483 <https://doi.org/10.3390/microorganisms8040600>
- 484 Branco, P., Francisco, D., Monteiro, M., Almeida, M. G., Caldeira, J., Arneborg, N., Prista, C., & Albergaria, H. (2017).
485 Antimicrobial properties and death-inducing mechanisms of saccharomycin, a biocide secreted by
486 *Saccharomyces cerevisiae*. *Applied Microbiology and Biotechnology*, *101*(1), 159–171.
487 <https://doi.org/10.1007/s00253-016-7755-6>
- 488 Ciani, M., & Comitini, F. (2015). Yeast interactions in multi-starter wine fermentation. *Current Opinion in Food*
489 *Science*, *1*, 1–6. <https://doi.org/10.1016/j.cofs.2014.07.001>
- 490 Combina, M., Elía, A., Mercado, L., Catania, C., Ganga, A., & Martinez, C. (2005). Dynamics of indigenous yeast
491 populations during spontaneous fermentation of wines from Mendoza, Argentina. *International Journal of*
492 *Food Microbiology*, *99*(3), 237–243. <https://doi.org/10.1016/j.ijfoodmicro.2004.08.017>
- 493 Curiel, J. A., Morales, P., Gonzalez, R., & Tronchoni, J. (2017). Different non-*Saccharomyces* yeast species stimulate
494 nutrient consumption in *S. cerevisiae* mixed cultures. *Frontiers in Microbiology*, *8*, 2121.
- 495 Del Fresno, J. M., Morata, A., Loira, I., Bañuelos, M. A., Escott, C., Benito, S., González Chamorro, C., & Suárez-Lepe, J.
496 A. (2017). Use of non-*Saccharomyces* in single-culture, mixed and sequential fermentation to improve red

497 wine quality. *European Food Research and Technology*, 243(12), 2175–2185.
498 <https://doi.org/10.1007/s00217-017-2920-4>

499 Englezos, V., Rantsiou, K., Cravero, F., Torchio, F., Pollon, M., Fracassetti, D., Ortiz-Julien, A., Gerbi, V., Rolle, L., &
500 Coccolin, L. (2018). Volatile profile of white wines fermented with sequential inoculation of *Starmarella*
501 *bacillaris* and *Saccharomyces cerevisiae*. *Food Chemistry*, 257, 350–360.
502 <https://doi.org/10.1016/j.foodchem.2018.03.018>

503 Fleet, G. H. (2003). Yeast interactions and wine flavour. *International Journal of Food Microbiology*, 86(1), 11–22.

504 Gobbi, M., Comitini, F., Domizio, P., Romani, C., Lencioni, L., Mannazzu, I., & Ciani, M. (2013). *Lachancea*
505 *thermotolerans* and *Saccharomyces cerevisiae* in simultaneous and sequential co-fermentation: A strategy to
506 enhance acidity and improve the overall quality of wine. *Food Microbiology*, 33(2), 271–281.
507 <https://doi.org/10.1016/j.fm.2012.10.004>

508 Gobert, A., Tourdot-Maréchal, R., Morge, C., Sparrow, C., Liu, Y., Quintanilla-Casas, B., Vichi, S., & Alexandre, H.
509 (2017). Non-*Saccharomyces* Yeasts Nitrogen Source Preferences: Impact on Sequential Fermentation and
510 Wine Volatile Compounds Profile. *Frontiers in Microbiology*, 8. <https://doi.org/10.3389/fmicb.2017.02175>

511 Heard, G. M., & Fleet, G. H. (1988). The effects of temperature and pH on the growth of yeast species during the
512 fermentation of grape juice. *Journal of Applied Bacteriology*, 65(1), 23–28. [https://doi.org/10.1111/j.1365-](https://doi.org/10.1111/j.1365-2672.1988.tb04312.x)
513 [2672.1988.tb04312.x](https://doi.org/10.1111/j.1365-2672.1988.tb04312.x)

514 Jolly, N. P., Varela, C., & Pretorius, I. S. (2014). Not your ordinary yeast: Non-*Saccharomyces* yeasts in wine
515 production uncovered. *FEMS Yeast Research*, 14(2), 215–237. <https://doi.org/10.1111/1567-1364.12111>

516 Kemsawasd, V., Branco, P., Almeida, M. G., Caldeira, J., Albergaria, H., & Arneborg, N. (2015). Cell-to-cell contact and
517 antimicrobial peptides play a combined role in the death of *Lachancea thermotolerans* during mixed-
518 culture alcoholic fermentation with *Saccharomyces cerevisiae*. *FEMS Microbiology Letters*, 362(14).
519 <https://doi.org/10.1093/femsle/fnv103>

520 Liu, Y., Forcisi, S., Harir, M., Deleris-Bou, M., Krieger-Weber, S., Lucio, M., Longin, C., Degueurce, C., Gougeon, R. D.,
521 Schmitt-Kopplin, P., & Alexandre, H. (2016). New molecular evidence of wine yeast-bacteria interaction
522 unraveled by non-targeted exometabolomic profiling. *Metabolomics*, 12(4), 69.
523 <https://doi.org/10.1007/s11306-016-1001-1>

- 524 Liu, Y., Rousseaux, S., Tourdot-Maréchal, R., Sadoudi, M., Gougeon, R., Schmitt-Kopplin, P., & Alexandre, H. (2017).
525 Wine microbiome: A dynamic world of microbial interactions. *Critical Reviews in Food Science and Nutrition*,
526 57(4), 856–873.
- 527 Mbuyane, L. L., de Kock, M., Bauer, F. F., & Divol, B. (2018). *Torulaspora delbrueckii* produces high levels of C5 and C6
528 polyols during wine fermentations. *FEMS Yeast Research*, 18(7), foy084.
- 529 Morata, A., Escott, C., Bañuelos, M. A., Loira, I., Del Fresno, J. M., González, C., & Suárez-Lepe, J. A. (2020).
530 Contribution of non-*Saccharomyces* yeasts to wine freshness. A review. *Biomolecules*, 10(1), 34.
- 531 Morgan, S. C., Haggerty, J. J., Jiraneek, V., & Durall, D. M. (2020). Competition between *Saccharomyces cerevisiae* and
532 *Saccharomyces uvarum* in Controlled Chardonnay Wine Fermentations. *American Journal of Enology and*
533 *Viticulture*, 71(3), 198–207.
- 534 Padilla, B., García-Fernández, D., González, B., Izidoro, I., Esteve-Zarzoso, B., Beltran, G., & Mas, A. (2016). Yeast
535 Biodiversity from DOQ Priorat Uninoculated Fermentations. *Frontiers in Microbiology*, 7.
536 <https://doi.org/10.3389/fmicb.2016.00930>
- 537 Petitgonnet, C., Klein, G. L., Roullier-Gall, C., Schmitt-Kopplin, P., Quintanilla-Casas, B., Vichi, S., Julien-David, D., &
538 Alexandre, H. (2019). Influence of cell-cell contact between *L. thermotolerans* and *S. cerevisiae* on yeast
539 interactions and the exo-metabolome. *Food Microbiology*, 83, 122–133.
540 <https://doi.org/10.1016/j.fm.2019.05.005>
- 541 Renault, Albertin, W., & Bely, M. (2013). An innovative tool reveals interaction mechanisms among yeast populations
542 under oenological conditions. *Applied Microbiology and Biotechnology*, 97(9), 4105–4119.
543 <https://doi.org/10.1007/s00253-012-4660-5>
- 544 Renault, Coulon, J., de Revel, G., Barbe, J.-C., & Bely, M. (2015). Increase of fruity aroma during mixed *T.*
545 *delbrueckii*/*S. cerevisiae* wine fermentation is linked to specific esters enhancement. *International Journal of*
546 *Food Microbiology*, 207, 40–48. <https://doi.org/10.1016/j.ijfoodmicro.2015.04.037>
- 547 Roca-Mesa, H., Sendra, S., Mas, A., Beltran, G., & Torija, M.-J. (2020). Nitrogen Preferences during Alcoholic
548 Fermentation of Different Non-*Saccharomyces* Yeasts of Oenological Interest. *Microorganisms*, 8(2), 157.
549 <https://doi.org/10.3390/microorganisms8020157>
- 550 Rollero, S., Bloem, A., Brand, J., Ortiz-Julien, A., Camarasa, C., & Divol, B. (2021). Nitrogen metabolism in three non-
551 conventional wine yeast species: A tool to modulate wine aroma profiles. *Food Microbiology*, 94, 103650.

- 552 Roullier-Gall, C., David, V., Hemmler, D., Schmitt-Kopplin, P., & Alexandre, H. (2020). Exploring yeast interactions
553 through metabolic profiling. *Scientific Reports*, *10*(1), 6073. <https://doi.org/10.1038/s41598-020-63182-6>
- 554 Roullier-Gall, C., Witting, M., Gougeon, R. D., & Schmitt-Kopplin, P. (2014). High precision mass measurements for
555 wine metabolomics. *Frontiers in Chemistry*, *2*, 102. <https://doi.org/10.3389/fchem.2014.00102>
- 556 Sadoudi, M., Tourdot-Maréchal, R., Rousseaux, S., Steyer, D., Gallardo-Chacón, J.-J., Ballester, J., Vichi, S., Guérin-
557 Schneider, R., Caixach, J., & Alexandre, H. (2012). Yeast–yeast interactions revealed by aromatic profile
558 analysis of Sauvignon Blanc wine fermented by single or co-culture of non-*Saccharomyces* and
559 *Saccharomyces* yeasts. *Food Microbiology*, *32*(2), 243–253. <https://doi.org/10.1016/j.fm.2012.06.006>
- 560 Seguinot, P., Englezos, V., Bergler, G., Brial, P., Ortiz-Julien, A., Brulfert, M., Camarasa, C., & Bloem, A. (2019). Non-
561 *Saccharomyces* yeast nitrogen consumption and metabolite production during wine fermentation. *OENO*
562 *2019 11th Symposium of Oenology*.
- 563 Snyman, C. (2019). *Impact of the protease-secreting yeast Metschnikowia pulcherrima IWBT Y1123 on wine*
564 *properties and response of protease production to nitrogen sources* [PhD Thesis]. Stellenbosch: Stellenbosch
565 University.
- 566 Snyman, C., Theron, L. W., & Divol, B. (2019). The expression, secretion and activity of the aspartic protease MpAPr1
567 in *Metschnikowia pulcherrima* IWBT Y1123. *Journal of Industrial Microbiology & Biotechnology*, *46*(12),
568 1733–1743. <https://doi.org/10.1007/s10295-019-02227-w>
- 569 Su, Y., Seguinot, P., Sanchez, I., Ortiz-Julien, A., Heras, J. M., Querol, A., Camarasa, C., & Guillamón, J. M. (2020).
570 Nitrogen sources preferences of non-*Saccharomyces* yeasts to sustain growth and fermentation under
571 winemaking conditions. *Food Microbiology*, *85*, 103287.
- 572 Wang, C., Mas, A., & Esteve-Zarzoso, B. (2016). The Interaction between *Saccharomyces cerevisiae* and Non-
573 *Saccharomyces* Yeast during Alcoholic Fermentation Is Species and Strain Specific. *Frontiers in Microbiology*,
574 *7*. <https://doi.org/10.3389/fmicb.2016.00502>
- 575 Williams, K. M., Liu, P., & Fay, J. C. (2015). Evolution of ecological dominance of yeast species in high-sugar
576 environments. *Evolution*, *69*(8), 2079–2093.

577
578
579 Figure Captions
580

581 **Figure 1: Single yeast fermentation discrimination.** Venn diagrams, principal component analysis and
582 hierarchical cluster of wine from single yeast fermentations (S, B, D and P) at the end of alcoholic
583 fermentation. The first two components represent 86.6% of variability. The cluster analysis followed by an
584 ANOVA with t-test (p-value 0.05) allowed the extraction of specific masses for each single fermentation
585 highlighted in the van Krevelen diagrams. The bubble sizes in the van Krevelen diagrams indicate relative
586 intensities of corresponding peaks in the spectra and bubble color represents chemical composition with
587 CHO containing compounds represented in blue, CHOS in green, CHON in red and CHONS in orange.

588 **Figure 2: Evolution of composition during the early stage of fermentation.** Mass difference network based
589 on the evolution of composition during fermentation from D, S and DS samples. 75.0% of assigned
590 molecular formulas could be connected in the network by allowing a set of 172 biological transformations.
591 Transformations are non-directed and correspond to edges in the graph. Compounds correspond to nodes
592 in the graph. In the first networks, nodes are colored according to their chemical composition: CHO in blue,
593 CHOS in green, CHON in orange and CHONS in red. In the other five networks, nodes are colored according
594 to their detection time during fermentation. Compounds already present in must are represented in
595 orange, then compounds detected after 24h fermentation are represented in yellow, after 48h in green,
596 after 72h in blue and after 96h in purple.

597 **Figure 3:** Impact of the S addition time. Hierarchical cluster of wine from single yeast fermentations (NS in
598 green and S in blue) and sequential fermentation (in pink) with Sc added at 24h, 48h and 72h at the end of
599 alcoholic fermentation.

600 **Figure 4: Impact of sequential fermentation on chemical composition.** Venn diagrams of wine at the end
601 of fermentation from single yeast fermentations (NS and S) and sequential fermentation with Sc added at
602 24h (NS24h), 48h (NS48h) and 72h (NS72h) with a Pie chart displaying the compounds common to NS and S
603 in single and sequential fermentations based on chemical composition (CHO in blue, CHOS in green, CHON
604 in orange and CHONS in red) and metabolic pathway (carbohydrates in pink, amino sugars in yellow, lipids
605 in green, amino acids and peptides in turquoise, polyphenols compounds in dark blue and unknown in
606 grey). Compounds classified as unknown refer to compounds not annotated in metabolic pathways.

607
608 **Table 1: Evolution of composition during the early stage of alcoholic fermentation.** Compounds detected
609 in the initial must and new compounds detected at 24h, 48h, 72h and 96h after the beginning of alcoholic
610 fermentation in samples from D, S and DS fermentations.

611